**NURETH14-397** 

# INTEGRATED PARTICLE IMAGING VELOCIMETRY AND INFRARED THERMOMETRY FOR HIGH RESOLUTION MEASUREMENT OF SUBCOOLED NUCLEATE POOL BOILING

X. Duan, J. Buongiorno and T. McKrell

Massachusetts Institute of Technology, Cambridge, Massachusetts, USA

#### **Abstract**

High-resolution data of nucleate pool boiling are important for the development of mechanistic numerical models based on computation fluid dynamics (CFD). This paper describes an innovative experimental facility that allows time- and space- resolved measurement of a series of important boiling-relevant quantities, including velocity and temperature distributions around individual bubbles, bubble shape, departure diameter and frequency, all of which can be used for validation of CFD-based models of boiling heat transfer. The facility comprises a temperature controlled boiling cell, with an indium tin oxide (ITO) heater and integrated high-frequency Particle Imaging Velocimetry (PIV) and Infrared Thermometry (IR). Some representative results are reported.

#### 1. Introduction

As an effective mode of heat transfer, nucleate boiling plays an important role in many energy and power systems, notably in light water reactors for nuclear power generation. Bubbles are formed on heated surfaces when the liquid immediately adjacent to the heated wall slightly exceeds the equilibrium saturation temperature. The process of liquid heating, nucleation, bubble growth and release is collectively referred to as the ebullition cycle. A detailed description of this process can be found in many publications (e.g. [1, 2]), and will not be repeated here.

Due to the complexity of the coupled fluid mechanics, energy transfer and bubble dynamics phenomena involved, prediction of nucleate boiling has been largely based on semi-empirical models. However, significant efforts are underway to develop more mechanistic computational fluid dynamics (CFD)-based models that can simulate the details of the bubble growth process [3-7]. The overall goal is to integrate such models into reactor thermal hydraulics codes, at first as closure models, ultimately as coupled simulations. The models make extensive use of interface tracking methods [8], which are being used to calculate the topology of the vapor-liquid interface and resolve the velocity and temperature gradients near the interface. Inspiration for and validation of these numerical models require experimental data of high fidelity and high spatial and temporal resolutions. In particular, the velocity and temperature distributions are needed along with the bubble size and shape throughout the ebullition cycle. The traditional experimental methods based on thermocouples and cameras can provide some, but not all of these information.

In recent years, many researchers have attempted to obtain high-resolution data of nucleate boiling. For bubble shape and volume, very high frame rate images of the bubble dynamics are

possible with rapid advances in high speed video cameras. For example, Kawara et al. [9] measured the volume-time evolution of a single vapor bubble at sub-cooled conditions with a resolution of 39 µs. These data were used by Ose and Kungi [6] to validate their numerical model on sub-cooled pool boiling. Non-intrusive flow field measurement in the presence of bubbles has been a tremendous challenge. In recent years, researchers have started to use the particle imaging velocimetry (PIV) technique for this purpose, mostly with air bubbles; only few studies with vapor bubbles. Cieslinski et al. [10] measured the flow field around single growing and rising vapor bubbles using PIV. Due to the very low frequency of their laser system (7.5Hz), the detailed transient features of the flow field were not captured. More recently, Dominguez-Ontiveros et al. [11] conducted PIV measurement of flow field in nucleate pool boiling of pure water and nano-fluids. A much higher acquisition rate (3600fps) was achieved. The authors showed averaged velocity profile and vorticity magnitude distribution in the flow field, but without details at the vapor-liquid interface or transient parameters during bubble growth or rising.

Heater surface temperature distribution is one of the most important parameters to be measured in boiling, as it relates directly to the local heat transfer coefficient. For detailed measurement beneath individual bubbles, the region to be investigated particularly the micro-layer region has an extremely small spatial dimension. Even the smallest available thermocouples would not be able to measure temperature profile of the micro-layer. A possible solution is to use thermochromic liquid crystals (TLC), as shown by Sodtke et al. [12] who conducted high resolution measurements of wall temperature distribution underneath a single vapor bubble. Since most TLCs can only work at low temperature ranges (often below 100 °C), the experiments with water are limited to either lower pressure, lower gravity, or other liquids with lower boiling point have to be used. Moreover the performance of unsealed TLCs deteriorates quickly in the presence of oxygen, solvents or lubricants. Due to these limitations with TLCs, many researchers have switched to infrared (IR) thermometry technique, such as Wagner and Stephan [13], and Gerardi et al. [14]. Kowalewski [15] did some preliminary work on simultaneous measurement of temperature and velocity fields around growing vapor bubbles by seeding the flow with TLCs. Using the standard PIV technique, the local velocity of the flow can be measured. In the mean time, the color change of TLCs reveals the temperature in the liquid. This seems to be an interesting method, although it is still limited by the drawbacks of TLCS described above. Currently, a commonly used approach is a combination of high speed video and high speed infrared thermometry, e.g. Wagner and Stephan [13] and Gerardi et al. [14]. Particularly in [14] the bubble departure diameter and frequency, growth and wait times, and nucleation site density were directly measured on the surface of an ITO heater where saturated pool boiling was sustained. However, so far there has been no research on integrated measurement of liquid velocity and heater surface temperature, i.e. a combination of PIV and infrared thermometry.

The objective of this study is to develop an experimental facility to provide synchronized data for fluid velocity around an individual bubble and wall temperature beneath the bubble, as well as nucleation site density, bubble departure diameter and frequency, bubble growth and wait times, and etc. We wish to use minimally-intrusive techniques (IR thermometry, high-speed video and PIV) and achieve high spatial and temporal resolutions. This paper describes the

challenges and solutions in developing such experimental capabilities, the details of the boiling facility, as well as some experimental results obtained from it.

# 2. Experimental method and apparatus

## 2.1 PIV challenges

Particle Image Velocimetry (PIV) is an effective experimental technique for non-intrusive measurement of velocity *fields* in fluid flow. In PIV the flow is seeded with small tracer particles that follow the flow. A targeted cross section of the flow is illuminated with a precisely controlled laser light sheet. A camera is used to record images of the particles in the illuminated plane. By tracking the displacement of the particles from frame to frame, it is possible to reconstruct the velocity field. Details on the working principle and practical applications of PIV can be found in [16].

Application of PIV in two-phase flow, particularly fluid flow with bubbles, is faced with several unique problems. With too many bubbles (void fraction >>1%) in the fluid, there is little space left for the tracer particles, which makes the velocity interrogation difficult. Moreover, the presence of bubbles that are of significant size (i.e. larger than a few hundred microns) will block the path of laser sheet and result in shadows in the particle images. Bubbles in front of the laser light plane will also block imaging for the camera. Keeping a low void fraction in the flow is the key. In the present study, we intend to measure fluid velocity around a single bubble. Ideally there should be only one bubble in each PIV images. In our boiling cell, bubbles are generated on a specially designed heater (detailed in the next section), the heat flux to which is precisely controlled at low levels so that only a few bubbles (less than 5 bubbles on a 10mm x 20 mm heated surface) are created at low frequency and nearly uniformly distributed on the heater surface. This leaves enough space in the fluid for PIV imaging. Even for a single bubble, a small shadow area may still be present in the light sheet behind the bubble. Fortunately in this study, flow field near a single bubble is usually axisymmetric and information on the half plan would be sufficient for validation of the numerical models.

Even with a single bubble in the fluid, conventional PIV technique still has imaging problems when the bubble size is significantly large (larger than a few hundred microns). The bubble can scatter/reflect a lot of light due to its Mie scattering. Too much laser light scattered from the bubble can damage the camera sensor. A large area around the bubble may appear as saturated white blank in the PIV images, impeding the velocity measurement. A solution to this problem is to seed the fluid with fluorescent particles. The wavelength of the fluorescence emitted from the seeding particles is longer than that of the reflected laser light. An optical filter is then used on the camera lens to block the scattered/reflected laser light while transmitting the fluorescence signal. The camera captures the fluorescence images of the seeding particles for PIV analysis. Such technique was used by Fujiwara et al. [17] in their measurement of bubble deformation and flow structure in a vertical channel. In our PIV system, we used 3 µm fluorescence tracer particles and a high-pass filter that has a small fraction (<0.5%) of residual transmission at 527nm (wavelength of our laser) to reveal the shape of the bubble.

## 2.2 The MIT boiling facility

Figure 1 shows a schematic of the pool boiling facility developed in this study. It includes a boiling cell, a high speed PIV system, a high speed infrared (IR) camera, and other auxiliary equipment. The PIV system consists of a high speed optical camera for imaging, an Nd-YLF laser system for flow illumination and a high speed controller. The controller allows for precisely timing control and synchronization of the laser, the optical camera, and the infrared camera. The optical camera can also work in the system without laser illumination and seeding particles in the boiling cell for high speed video (HSV) images. All the important parts of this facility are described next.

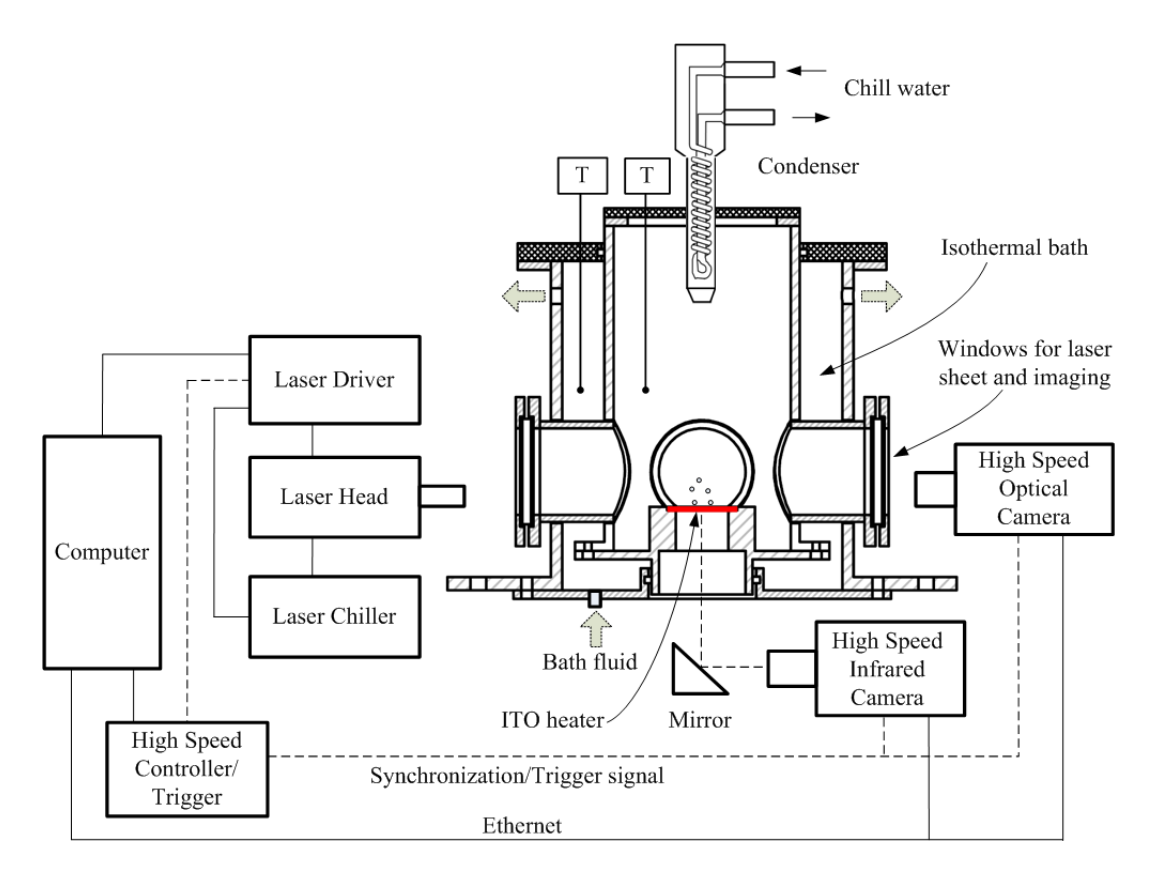


Figure 1 Schematic of the boiling facility with PIV and infrared thermometry systems.

#### (1) Boiling cell

The boiling cell features a concentric-double- cylinder structure: boiling of deionized (DI) water takes place in the inner cell, while the outer enclosure functions as an isothermal bath. Saturated or sub-cooled boiling conditions in the inner cell can be controlled (with 0.1°C precision) by circulating a temperature-controlled fluid through the isothermal bath. A heater sample support unit sits at the bottom of the boiling cell. It allows for an ITO heater to be installed on the top of it, while leaving an optical access to the bottom of the ITO heater (for measurement with the IR camera) from below the boiling cell. The whole heater support unit is designed to be immersed in the isothermal bath, which minimizes heat losses from the ITO heater sample to the support unit. There are four glass windows spaced equally at 90° along the outer surface of the boiling cell. Two adjacent windows are for the laser illumination and imaging of the PIV system. A

condenser is installed through a hole in the center of the inner cell cover to prevent fluid loss in the boiling cell. Thermocouples are inserted into the inner cell and the isothermal bath to monitor the temperatures. All the metal parts are made from stainless steel 316 to prevent corrosion. The boiling cell has four legs with wheels for support and adjustment purposes.

#### (2) ITO heater

Boiling occurs on a specially designed heater installed in the inner boiling cell. Figure 2 shows one of several possible designs. The heating element is an ITO layer of 0.7  $\mu$ m thickness vacuum deposited onto a 0.25 mm thick sapphire substrate. The sapphire substrate has a size of 50mm x 50mm, while the exposed heating area of ITO is 10 x10 mm<sup>2</sup>. Silver electrode pads of 20  $\mu$ m are used for DC power supply to the heater.

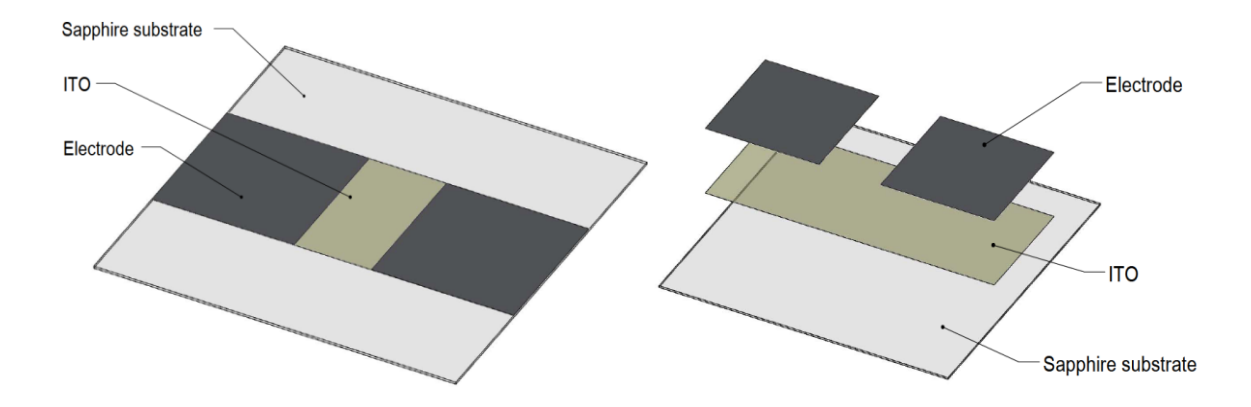


Figure 2 Schematic of the ITO heater.

The heater is installed on the heater support unit and sealed with a sticky silicone-gel. The ITO heating element is in contact with the water and is resistively heated. In the experiments, voltage and current across the ITO heater is measured and the actual heat flux through the ITO heater is thereby monitored in the data acquisition system. The bottom surface of the sapphire substrate is exposed to air. The ITO is transparent in the visible range (380-750nm), but opaque in the mid-IR (3-5µm) range, while the sapphire substrate is transparent in both the visible and mid-IR ranges. This combination allows temperature measurement on the bottom of the ITO layer with the high speed IR camera. Because the ITO heater is so thin, the temperature drop across the ITO is negligible, so we measure the temperature right where boiling occurs.

## (3) PIV system

In the PIV system, a high repetition Nd:YLF laser (Photonics Industries, Model DM20-527) is used to illuminate the fluid. A compact infinitely adjustable light sheet optics unit on the laser head produces a visible green (527 nm wavelength) laser sheet less than 0.5mm thick. The laser has pulse energy of 20mJ at 1000Hz, with pulse duration of 180ns. The pulse repetition rate can be up to 10 kHz, although 1000Hz was used in most of our PIV measurement (with some experiments running at 3000 Hz and 5000Hz). The fluid in the inner boiling cell is seeded with a type of fluorescent particles- Fluoro-Max, polymer microspheres of 3.2 μm. A Phantom 12.1 high speed video camera (Vision Research) is used for imaging the boiling process. The camera's CMOS sensor is 25.6 mm x 16.0 mm with 20 μm pixel size. An AF Micro-Nikkor 200mm f/4D lens (Nikon) is used for "close-up" imaging of the flow fields around a single

bubble. The long working distance (260mm) of this lens allows the camera to reach its 1:1 reproduction rate with a safe distance from the hot boiling cell, since the distance from the ITO heater to outer edge of the windows of the boiling cell is only 137mm. If this best magnification is kept during the imaging process, the images will always have a 20  $\mu$ m/pixel scale. This leads to a 20  $\mu$ m spatial resolution in analyzing the HSV images and a maximum field of view (FOV) of 25.6 mm x 16.0 mm in the flow field. When extension rings are used for the camera lens, even better magnification can be achieved. The PIV analysis software DaVis 7.2 (LaVision) is used for imaging and velocity analysis. It also enables setup of the high speed controller to control the timing of the laser and high speed cameras. In the velocity analysis, interrogation area size of 32 x 32 pixels is mainly used in our measurement, with 50% overlap for cross correlation. This gives a spatial resolution of 0.64mm for the velocity vectors.

#### (4) IR camera and IR thermometry

A SC6000 high-speed infrared camera (FLIR Systems) is used to record the temperature distribution on the heater surface. The sensor of the IR captures mid-IR (in the 3-5 $\mu$ m wavelength range) radiation from the ITO heater surface, which is reflected to the view of IR camera through a golden mirror, as shown in Fig.1. A 100mm germanium lens (f/2.3) with a 3/4" extension ring was used to achieve the desired spatial resolution at the optimal camera distance from the reference plane. A spatial resolution of 0.1mm was achieved in the experiments. The details of the IR camera are described in [14], along with the procedure and accuracy of the temperature measurement. Basically the camera sensor detects the infrared radiation intensity and outputs the signal as pixel counts. The calibration leads to a counts-temperature curve to be used for conversion of the intensity image to temperature fields.

The IR camera has a maximum resolution of 640 x 512 pixels. The maximum frame rate is dependent on the imaging window size; for a full frame 640 x 512 window, this is 126 Hz. In the experiment, only a small window (e.g. 224 x 116) is needed for imaging the whole ITO heater surface, allowing for a high frame rate of 1000fps. For measurement of a single bubble, even higher frame rate can be achieved; frame rates up to 3000fps were used in the experiment.

Table 1 summarizes the measurement capabilities of the individual equipment, HSV, Infrared and PIV. Note that for synchronized PIV and IR measurement the temporal resolution is limited by the IR camera- up to 3000 fps for measurement of a single bubble.

Table 1 Measurement capability of the boiling facility

Parameters and	Bubble dimensions	Surface temperature	Liquid velocity
requirements	(HSV)	(IR)	(PIV)
Range	0.1mm - 12mm	50-120 °C	6 mm/s - 1m/s
Spatial resolution	20 μm	0.1mm	0.64 mm
Temporal resolution	0.2ms - 1ms	0.34 ms	0.5 ms - 1ms
Accuracy	80 μm	2°C	1%

## 2.3 Experimental procedure

The ITO heater is installed onto the heater support unit. The inner boiling cell is cleaned and then filled with distilled water or DI water. The circulation heater is set to the desired temperature for the isothermal bath. It usually takes up to 65 minutes to heat up the boiling cell from room

temperature to 100°C and degas it. Then the ITO heater is powered to reach the desired heat flux for nucleate boiling. The IR camera is focused to the ITO heater plane and its imaging window is setup to include a chosen bubble. When the laser is used, the positioning and distance between the laser head and the ITO heater should be adjusted so that (1) the laser sheet is illuminating the plane of the chosen nucleation site, and (2) the waist of the laser sheet (where it is the thinnest) is just above the nucleation site. This ensures good illumination and therefore imaging of the bubble behaviors. PIV and IR imaging are started when cyclic conditions are reached in the boiling process - after several ebullition cycles of the bubble.

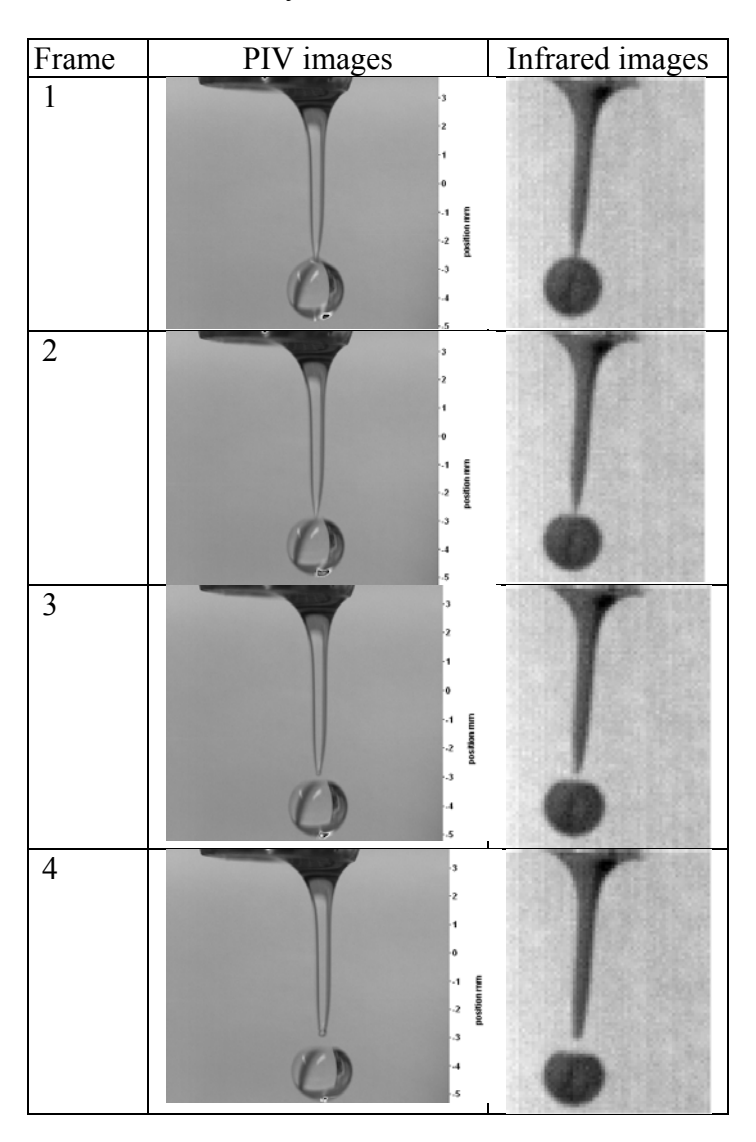


Figure 3 Comparison of synchronized PIV and Infrared images.

The high speed controller produces transistor-transistor logic (TTL) pulses (with desired frequency set in the DaVis software) which trigger both the IR and PIV system to simultaneously record IR and PIV images, allowing the synchronization of both cameras' image sequences. Alternatively, the IR camera can send out a trigger signal to the PIV system for the

synchronization. Figure 3 shows a comparison of the synchronized PIV and IR images at 1000 Hz (i.e., each frame is 1ms apart) in a water droplet test.

#### 3. Results and discussions

The following data are reported: (1) time-resolved HSV data of dimensions/shape variation of a bubble in nucleate boiling of sub-cooled water, (2) velocity field around a growing and rising bubble from PIV measurement, and (3) high resolution IR measurement of heat surface underneath a single growing bubble.

#### (1) HSV measurement of bubble growth and rising in sub-cooled water

Figure 4 shows the variation of bubble dimensions and vertical locations in sub-cooled boiling of water at atmospheric pressure. The bulk water temperature was kept at  $96.1^{\circ}$ C, and the heat flux from ITO was  $40.2 \text{kW/m}^2$ . High speed video images of the bubble were taken at 5000 fps. The vertical dimension,  $D_{bv}$ , and horizontal dimension,  $D_{bh}$  of the bubble were measured along with the distance from the bottom tip of the bubble to the heater surface,  $H_{bb}$ . The latter will indicate the bubble's vertical location and velocity of rising. Following Dong et al. [18], the aspect ratio E, and equivalent diameter,  $D_{eq}$ , of the bubble shape are defined as

$$E = \frac{D_{b\nu}}{D_{bh}} \tag{1}$$

$$D_{eq} = \sqrt[3]{D_{bv} \times D_{bh}^2} \tag{2}$$

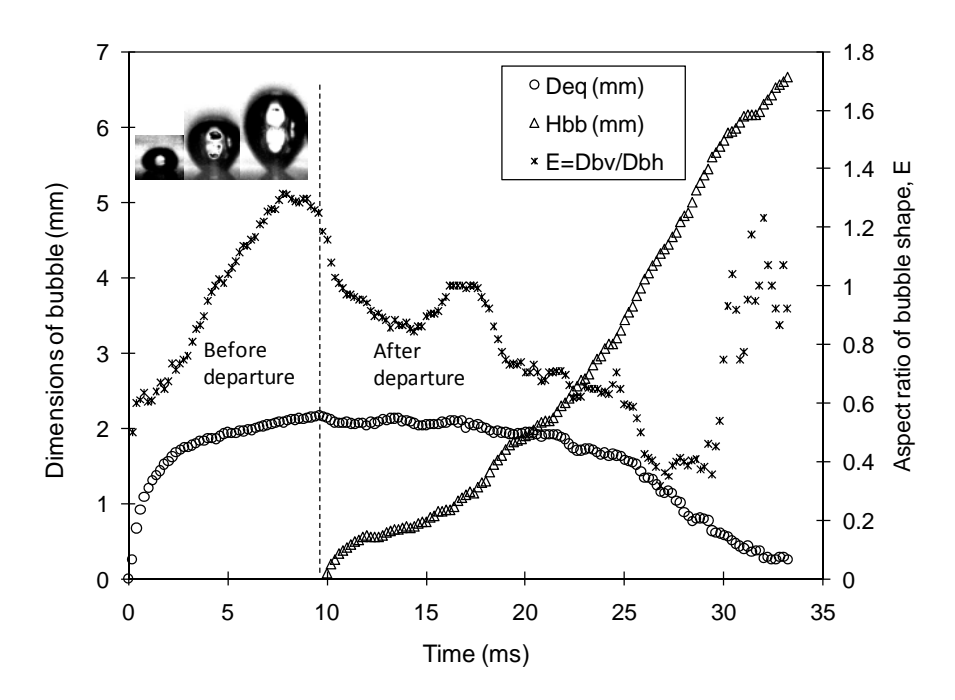


Figure 4 Bubble dimensions and vertical locations in sub-cooled boiling of water.

Three typical bubble pictures are shown here at 0.4ms, 4.8ms, 8ms of bubble growth. The initial shape is hemispherical (with E around 0.5) during the inertia-controlled growth period, and later

spherical (E around 1) during the heat transfer-controlled growth period.

## (2) Velocity field around a vapor bubble

Figure 5 shows velocity fields around a vapor bubble during its growing and rising process. The length and color of the vectors indicate the magnitude of velocity and the arrow indicate the direction of liquid flow. The measurements were conducted with DI water under saturated nucleate boiling conditions. Heat flux of the ITO heater was 36.5 kW/m<sup>2</sup>. The vapor bubble was generated at a frequency of 12/second.

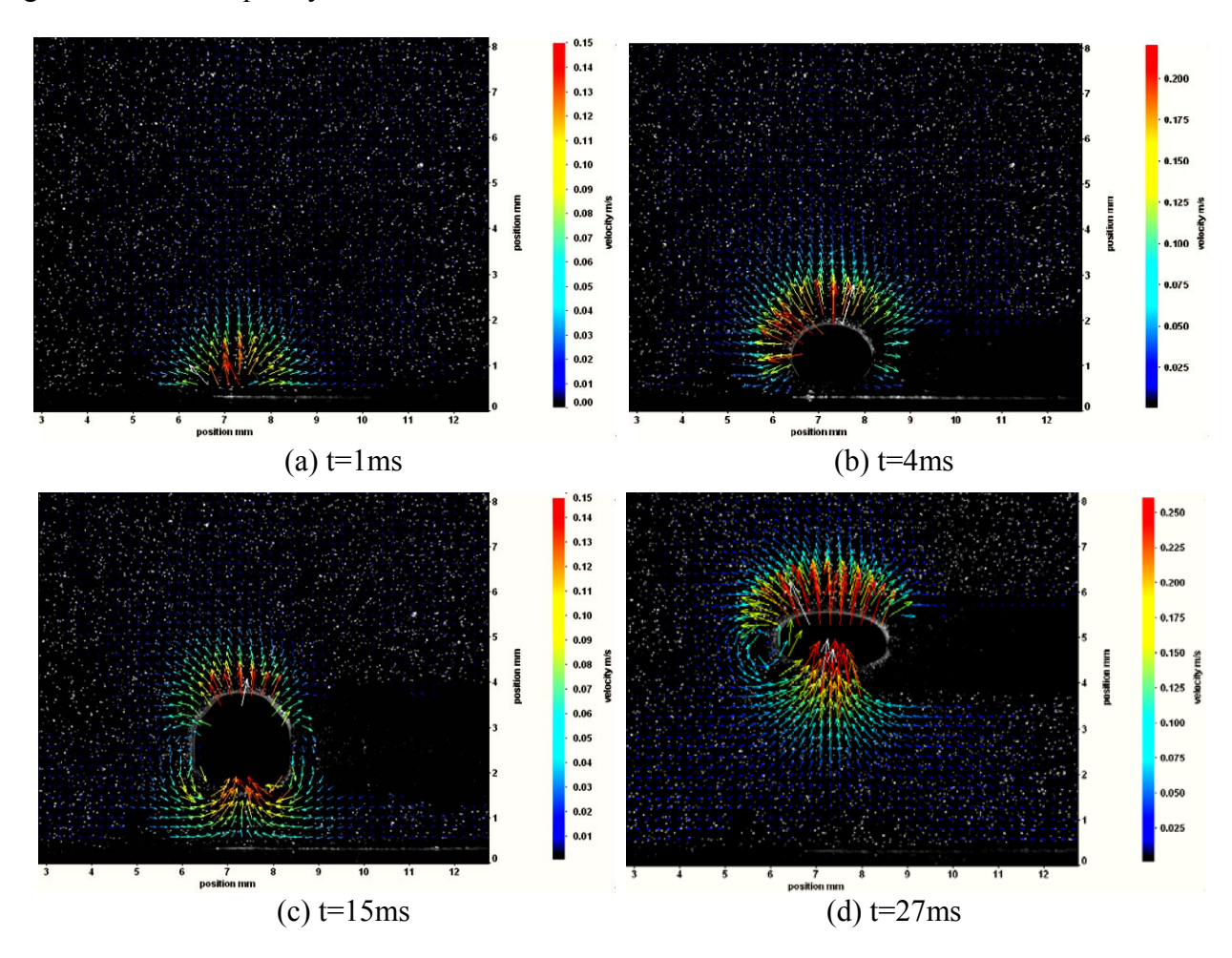


Figure 5 Velocity fields around a growing and rising bubble.

These preliminary PIV measurements have shown that under the experimental conditions (particularly low heat flux, only 1 or 2 individual bubbles) significant velocity fields exist only in a limited space around the bubble. The diameter of this space is approximately twice of that of the bubble. Beyond this "disturbed space", the liquid is almost quiescent, with velocities lower than 0.01m/s, as compared to a maximum velocity of 0.32m/s immediately around the bubble. In addition, it can be confirmed that the fluid comes to an almost complete standstill after a bubble departs and before a new bubble is formed. This corroborates an assumption typically made in the numerical simulations that the initial velocity is zero throughout the domain.

#### (3) Sample IR results

High speed IR measurement enables detailed investigation of the heater surface temperature variation beneath a growing bubble. Figure 6a shows an example with a high frame rate (2975fps). Variation of the blue (darker) ring indicates the variation of the micro-layer width. Fig. 6b is a plot of the temperature distribution with time; the solid curves indicate temperature decrease with time and dashed curves indicate temperature regain with time.

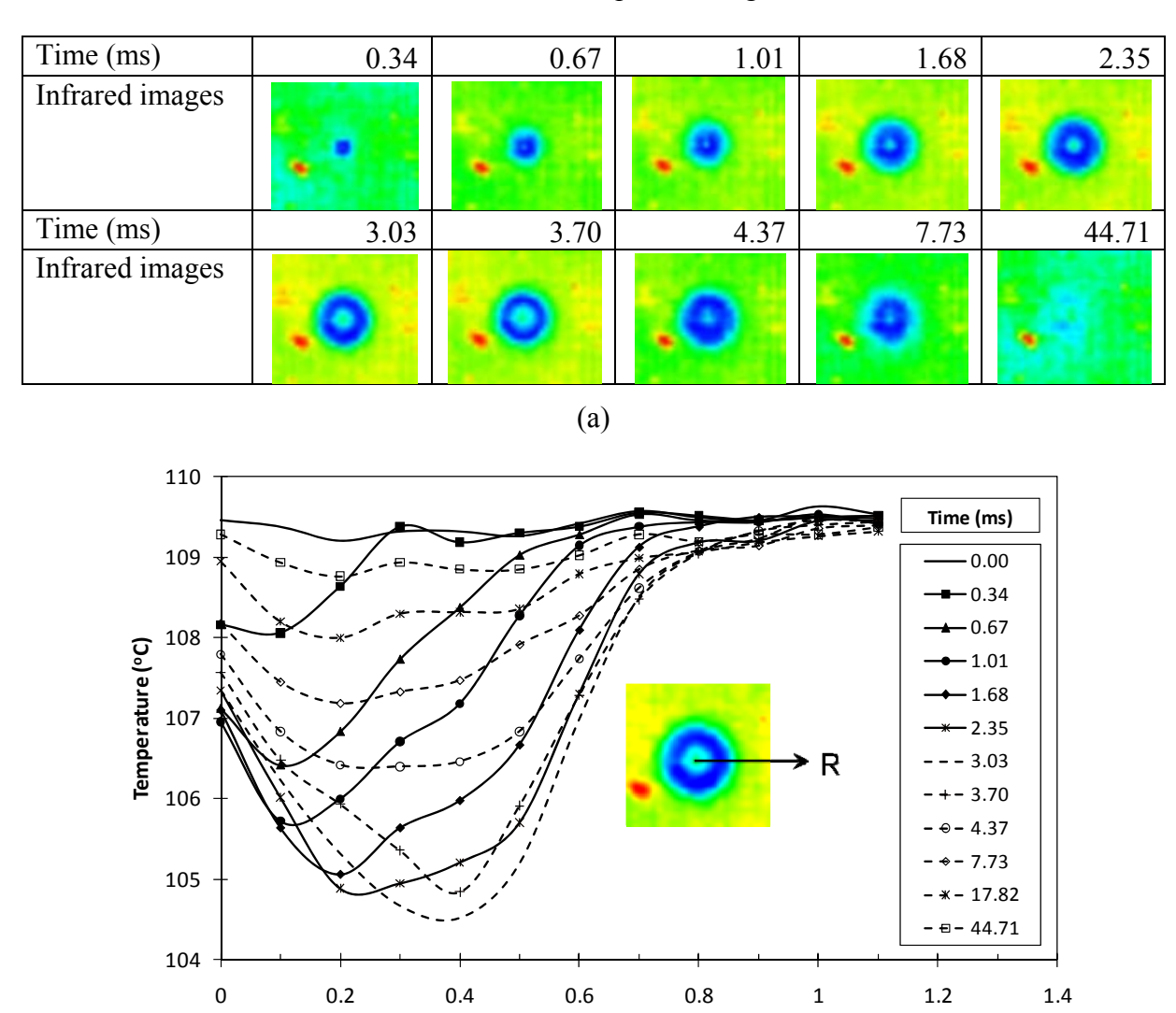


Figure 6 Heater surface temperature distribution during bubble growth.

(b)

R(mm)

#### 4. Conclusion

A new facility for investigation of nucleate boiling phenomena at saturated and sub-cooled conditions was presented. With integrated high-speed video, PIV and IR thermometry, this facility is capable of non-intrusively generating time- and space-resolved data for key nucleate boiling parameters, including bubble departure diameter and frequency, velocity and temperature

fields around and beneath the bubble. These data can be used to gain insight into the fundamentals of nucleate boiling, and, more importantly, for validation of mechanistic models of boiling, including CFD-based models. We are currently adding laser induced fluorescence (LIF) capabilities [17, 19] to the facility, to enable measurement of the temperature field within the fluid, not only on the heater surface.

#### 5. References

- [1] V. Carey, *Liquid-Vapor Phase Change Phenomena*, 2nd Edition, Taylor & Francis, New York, USA, 2008.
- [2] J. Kim, "Review of nucleate pool boiling bubble heat transfer mechanisms", *International Journal of Multiphase Flow*, 2009, Vol. 35, no.12, pp.1067-1076.
- [3] V.S. Nikolayev, D.A. Beysens, G.L. Lagier, J. Hegseth, "Growth of a dry spot under a vapor bubble at high heat flux and high pressure", *International Journal of Heat and Mass Transfer*, 2001, Vol.44, No.18, pp. 3499-511.
- [4] G. Son, N. Ramanujapu, V.K. Dhir, "Numerical simulation of bubble merger process on a single nucleation site during pool nucleate boiling", *Journal of Heat Transfer*, 2002, Vol.124, No.1,pp. 51-62.
- [5] G. Tryggvason, S. Thomas, "Direct numerical simulations of nucleate boiling", Proceedings of IMECE-2008, October 31-November 6, 2008, Boston.
- [6] Y. Ose, T. Kunugi, "Numerical simulation on subcooled pool boiling", Paper No. MN-10, 6th International Symposium on Multiphase Flow, Heat Mass Transfer and Energy Conversion, Xi'an, China, 11-15 July 2009.
- [7] C. Kunkelmann, P. Stephan, "CFD simulation of boiling flows using the volume-of-fluid method within OpenFOAM", <u>ECI International Conference on Boiling Heat Transfer</u>, Brazil, May 3-7, 2009.
- [8] G. Tryggvason, R. Scardovelli, S. Zaleski, *Direct Numerical Simulations of Gas-Liquid Multiphase Flows*, Cambridge University Press, 2011.
- [9] Z. Kawara, T. Okota, and T. Kunugi, "Visualization of behavior of subcooled boiling bubble with high time and space resolutions", <u>Proceeding of the 6th pacific symposium on flow visualization and image processing</u>, 2007, pp. 424-428.
- [10] J. T. Cieslinski, J. Polewski, J. A. Szymczyk, "Flow field around growing and rising vapor bubble by piv measurement", *Journal of Visualization*, Vol. 8, No. 3, 2005, pp.1343-8875
- [11] E. Dominguez-Ontiveros, S. Fortenberry, and Y. A. Hassan, "Experimental observations of flow modifications in nanofluid boiling utilizing particle image velocimetry", *Nuclear Engineering and Design*, Vol.240, No. 2, 2010, pp. 299-304.
- [12] C. Sodtke, J. Kern, N. Schweier, and P. Stephan, "High resolution measurements of wall temperature distribution underneath a single vapor bubble under low gravity conditions", *International Journal of Heat and Mass Transfer*, 2006, Vol.49, pp.1100-1106.
- [13] E. Wagner, and P. Stephan, "High-resolution measurements at nucleate boiling of pure FC-84 and FC-3284 and its binary mixtures", *ASME Journal of Heat Transfer*, Vol. 131, 2009, 121008.

- [14] C. Gerardi, J. Buongiorno, L. Hu, T. McKrell, "Study of bubble growth in water pool boiling through synchronized, infrared thermometry and high-speed video", *International Journal of Heat and Mass Transfer*, 2010, Vol. 53, no.19-20, pp. 4185-4192.
- [15] T.A. Kowalewski, "Particle image velocimetry and thermometry for two-phase flow problems", *Annals of the New York Academy of Sciences*, 2002, Vol. 972, pp.213–222.
- [16] M. Raffel, C. E. Willert, S. T. Wereley, J. Kompenhans, *Particle Image Velocimetry-A Practical Guide*, Second Edition, Springer Berlin Heidelberg New York, 2007.
- [17] A. Fujiwara, Y. Danmoto, K. Hishida, M. Maeda, "Bubble deformation and flow structure measured by double shadow images and PIV/LIF", *Experiments in Fluids*, Vol. 36, 2004, pp.157–165.
- [18] H. Dong, X. Wang, L. Liu, X. Zhang, S. Zhang, "The rise and deformation of a single bubble in ionic liquids", *Chemical Engineering Science*, vol.65, 2010, pp.3240-3248.
- [19] M. C. J. Coolen, R. N. Kieft, C. C. M. Rindt, A. A. van Steenhoven, "Application of 2-D LIF temperature measurements in water using a Nd:YAG laser", *Experiments in Fluids*, 1999, Vol. 27, No.5, p.420-426.